Modified Particle Swarm Optimization Based on Lead-Lag Power System Stabilizer for Improve Stability in Multi-Machine Power System

Nader M.A. Ibrahim[1], Basem E. Elnaghi[2], Hamed A. Ibrahem[3], and Hossam E.A. Talaat[4]

[1]Electrical Department, Faculty of Industrial Education, Suez University, Suez, Egypt
[2]Electrical Engineering Department, Faculty of Engineering, Suez Canal University, Ismailia, Egypt
[3]Electrical Department, Faculty of Industrial Education, Suez University, Suez, Egypt
[4]Electrical Engineering Department, Faculty of Engineering-Ain Shams University, Cairo, Egypt

Nader.Ibrahem@suezuniv.edu.eg, basem.elhady@gmail.com, hamed_4a@yahoo.com, hossamtalaat@hotmail.com

Abstract: Inter-area oscillations not only limit the transferred bulk power but can extend to isolate the areas and may cause the blackout in some parts of the system or all the system. This paper depicts the improvement process of power system stability by using the modified particle swarm optimization (PSO) technique to optimize the lead-lag power system stabilizer (PSS) parameters offline to improve its performance. PSO modified by adjusting the damping boundary condition to prevent the particles from an outing of the searching space which improves the optimization process. Optimized PSS structure is a conventional lead-lag PSS (IEEE type-PSS1A) with speed deviation input signal. Proposed PSS performance compared with bacterial foraging based lead-lag PSS, and a simplified multi-band PSS: IEEE® type PSS4B. A comparison process applied to the system divided into two areas 11-bus 4-generators. Furthermore, performance indices as Eigenvalue, damping ratio, participation factor, maximum overshoots, settling time, and steady-state error used to utilize the analysis. The simulation results clarify the strength of the proposed PSS over the other compared PSSs. Simulation results in mathematical analysis prove that the proposed PSS improves the overall system stability better than the BG based lead-lag PSS by (23.02835%) and the MB-PSS by (94.14835%).

Keywords: artificial intelligence techniques, modified PSO, bacterial foraging, multi-machine power system stability, power system stabilizer optimization, inter-area oscillation.

1. Introduction

The electric power systems structure grows swiftly, which involve a large number of devices as generators, controllers, transmission lines, transformers, and loads. Interference among these devices makes the system complicated and its constructing vulnerable to instability problem. Power system stability signifies the system aptitude to remain stable after any disturbance [1].

Stability problems categorized into three sets of rotor angle stability, frequency stability, and voltage stability. Rotor angle stability involved with the interconnected synchronous generators to run synchronized under normal operation situation and after a large and a small disturbance [2].

Small disturbances like load change require the system to adjust within the varying conditions to serving the loads satisfactorily. The large disturbance like the short circuit or a transmission line and huge generators fail. If the system still stable it will return with a new equilibrium operating point. On the contrary, if the system is unstable when a generator goes out of synchronizing. Consequently, the instability in one part may lead to small parts outages then blackout [1, 2].

Small signal rotor angle stability classified into local, inter-area, control, and torsional modes. Inter-area modes defined by the swinging of arranged machines in one region against another machines assortments in the system. The inter-area oscillation created when two or numerous groups of a faithfully attached generator interconnected by a long weak transmission line waving against each other [3].

Received: December 25th, 2018. Accepted: March 18th, 2019
DOI: 10.15676/ijeei.2019.11.1.10

Inter-area oscillation must dump immediately by the power system stabilizer (PSS), which recognized the efficient controller to damp the LFOs. PSSs works to add damping to the generator rotor oscillation by adding its stabilization signal to the generator excitation, which increases the AVR ability in damping the inter-area oscillation and improves the overall system stability [2].

Researchers work on improving the PSS strength and enhance the PSS strength in damping the LFOs. An enormous method used to develop the PSS strength. PSS design based on a mathematical model such as a point wise min-norm control law and a third-order state-space calculated the model of the synchronous generator [4], improved Teaching-Learning Algorithm (TLA) by the chaotic map [5].

Adding control devices in coordination with the optimized PSS on the system to develop the power system stability similar to using a new optimization algorithm-based method of Fuzzy Adaptive Bacterial Foraging (FABF) used to design PSS and the Controlled Series Capacitor (TCSC) for damping the LFOs [6], and apply coordination between proportional-integral-derivative (PID-PSS) enhanced by Firefly (FF) with the static synchronous series compensator (SSSC) [7].

Using artificial intelligence (AI) techniques in designing PSS used in two ways. Firstly, by implementing the AI as the PSS similar to advanced power system stability controller (SPSSC) using Neuro-fuzzy system [8], optimize a fuzzy logic-PSS by an adaptive neuro-fuzzy inference system (ANFIS) [9], and deciding a fuzzy PSS parameter using the particle swarm optimization (PSO) [10].

Secondly, Using AI technique in optimizing the PSS parameters offline means before the enforcement of the PSS in the system like using tune the parameters of FLPID using PSO [11], optimize PID-PSS by using PSO and the genetic algorithm (GA) [12], applying hybrid PSO (HPSO) to tune the PSS parameters [13], the Firefly Algorithm to design the PSS [14], using the combination of the dynamic GA (DGA) with PSO techniques to optimize the fractional-order multi-band PSS (Fo-MB-PSS) [15], using the PSO to adjust the optimal model reference adaptively system (MARS) which used to improve the lead-lag PSS [16].

The last-mentioned methods which depend on AI techniques to optimize the CPSS parameters offline are the simplest by relying on the CPSS simplicity without adaptation or tuning during system operation, which delays the action of the PSS. In this study the modified PSO used for tuning the lead-lag parameters to improve its performance in damping the inter-area oscillation and the overall system stability.

MatSim defined as A Multi-machine Small-signal Stability program package used to analyze and indicate the system state. The proposed PSO based lead-lag PSS tested with large and small signal criteria in two areas multi-machine power system. This comparison with bacterial foraging based lead-lag (IEEE type-PSS1A) PSS the same structure, and multi-band PSS simplified settings: IEEE® type PSS4B according to IEEE Std. 421.5. Prove the proposed PSS superiority to the other PSSs.

Paper summaries: Section II power system model and PSS structure. Section III power system analysis. Section IV optimization technique. Section V simulation. Finally, section VI conclusion.

2. Power System Model and PSS Structure

A. Power System Model

The power system model which used as a simulation problem is P. Kundur 4 machine -11 bus two-area power system. Figure 1 shown the one-line diagram of the system which its full details illustrated in [17].

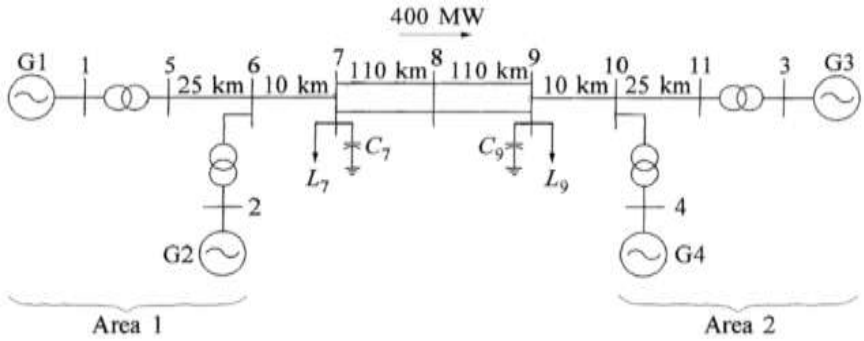

Figure 1. The one-line diagram of two areas 4-machine 11-bus.

The multi-machine system model expressed as a differential equation, which produced from different devices that connected to the system like generators, the excitation systems, and the controllers. In this work, the generators modeled by d-q axis using 6-order model, and described by the following six differential equations [18]:

$$\delta'_i = \omega_{ri} - \omega_{oi} \tag{1}$$

$$\omega_{ri} = \frac{(P_{mi} - P_{ei} - D_i(\omega_{ri} - 1))}{M_i} \tag{2}$$

$$e'_{qi} = \frac{\left(-e'_{qi} - \left(X_{di} - X'_{di} - \frac{T''_{doi} X''_{di}}{T'_{doi} X'_{di}}(X_{di} - X'_{di})\right) i_{di}\right)}{T'_{doi}} \tag{3}$$

$$e'_{di} = \frac{\left(-e'_{di} + \left(X_{qi} - X'_{qi} - \frac{T''_{qoi} X''_{qi}}{T'_{qoi} X'_{qi}}(X_{qi} - X'_{qi})\right) i_{qi}\right)}{T'_{qoi}} \tag{4}$$

$$e''_{qi} = \frac{\left(-e''_{qi} + e'_{di} - \left(X'_{di} - X''_{di} - \frac{T''_{doi} X''_{di}}{T'_{doi} X'_{di}}(X_{di} - X'_{di})\right) i_{di}\right)}{T''_{doi}} \tag{5}$$

$$e''_{di} = \frac{\left(-e''_{di} + e'_{di} + \left(X'_{qi} - X''_{qi} - \frac{T''_{qoi} X''_{qi}}{T'_{qoi} X'_{qi}}(X_{qi} - X'_{qi})\right) i_{qi}\right)}{T''_{qoi}} \tag{6}$$

All generators associate with tandem compound single reheat prime-mover and the steam turbine connected to speed governing system. Speed governor and the steam turbine details clarified in the IEEE committee report [19].

Figure 2 (A & B) shown the speed governor system for the steam turbine, and the tandem compound, single reheat prime mover steam turbine respectively. The voltage regulator type is DC1A excitation system model shown in figure 3. The details of the regulator revealed in the IEEE excitation model report IEEE Std. 412.5-2005 [20].

The Heffron-Philips block diagram for the multi-machine power system without PSS showed in figure 4, which firstly proposed in [21]. The constants are the interaction between the generators; the constants equations proved & discussed in [22].

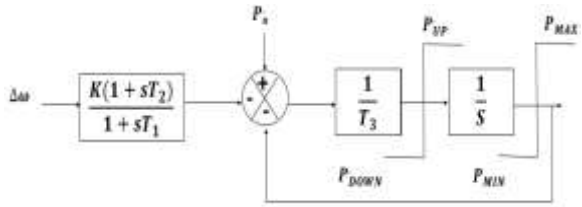

(A)

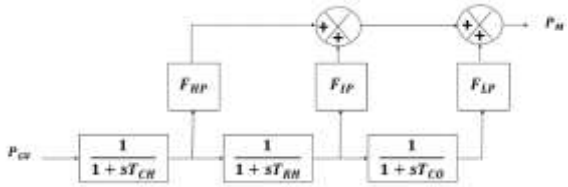

(B)

Figure 2. The dynamic models of (A) The speed governor system for steam turbine & (B) The tandem compound, single reheat prime mover steam turbine.

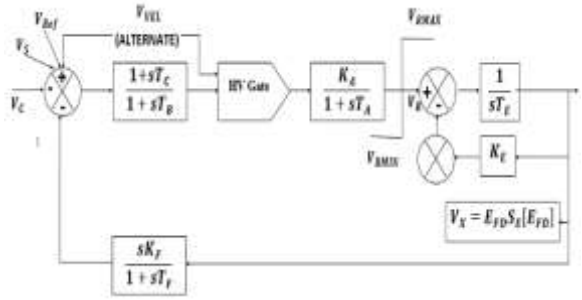

Figure 3. Type-DC1A-DC commutator exciter.

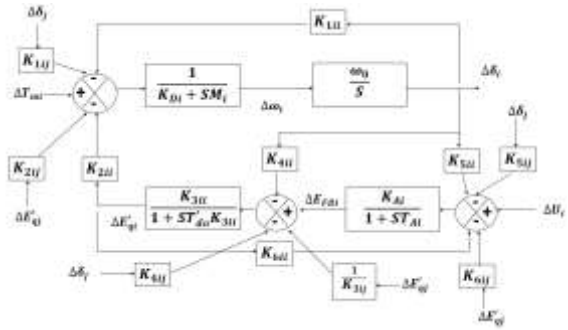

Figure 4. Heffron–Phillips block diagram of multi-machine power system without PSS.

B. Power System Stabilizer

The function of the power system stabilizer (PSS) is to add damping torque according to the generator rotor oscillation by adding it to the AVR signal in the generator excitation system [17]. In this paper, the IEEE type-PSS1A PSS with speed deviation as input signal shown in figure 5, and the stabilizer data described in [17].

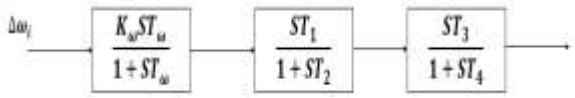

Figure 5. The block diagram of IEEE type-PSS1A (Lead-Lag) PSS.

3. Power System Analysis

The power system analysis process depends on The MatSim a Multi-Machine Small-signal Stability Package which used as a MATLAB/Simulink-based Single-Line Editor for Small-signal Stability Analysis created by Ajay Pai P., and available as an open-source framework at [23]. The MatSim is a MATLAB toolbox used for mathematical and dynamic analysis of the electric power system. The MatSim has its built-in library to draw the power system in a single-line diagram.

Table 1 shows the summarized Eigenvalue analysis of the system state matrix which computed by MatSim toolbox and the dominant state variable that has high participation value in each mode.

Table 1. System modes without PSS.

Eigenvalues		Frequency	Damping Ratio	Most Associated States
Real	Imaginary			
-0.04888	±9.9753	1.5876	0.0049	$\Delta\omega_2, \Delta\delta_2$
-0.05028	±10.28836	1.6374	0.0049	$\Delta\omega_4, \Delta\delta_4$
-0.00322	±3.74788	0.5965	0.0008	$\Delta\omega_3, \Delta\delta 3$

Table 1 demonstrates that the system without PSS suffers from an inter-area mode has a frequency with 0.5965 Hz., plus damping ratio 0.0008, and two local modes with frequency 1.5876, & 1.6374 and damping ratio 0.0049, & 0.0049 respectively.

Figure 6 displays the mode shape graph, which drawn from the Right-Eigenvalues at each dominant form. This figure manifest that the system is unstable when analyzing the local mode with 1.587 Hz during generator G1 swings against G2 within region 1. Also, the local mode that has a 1.6374 Hz frequency generated while the G3 swing versus G4 inside zone 2. Moreover, the third mode produced a frequency 0.5964 Hz is an inter-area mode begun when generators G1 & G2 from area 1 swing toward G3 & G4 in zone 2.

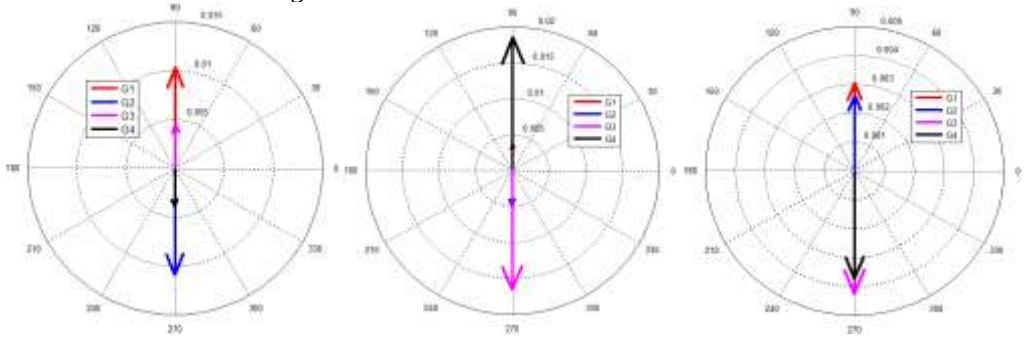

(A) Local mode $f = 1.5876Hz, \xi = 0.00490$

(B) Local mode $f = 1.6374Hz, \xi = 0.004887$

(C) Local mode $f = 0.5964Hz, \xi = 0.00085$

Figure 6. The swing modes compass plot.

The inter-area mode with damping ratio 0.00085 is the most danger stability problems of the three swing modes because this mode wouldn't be stable without the reaction of robust PSS against this LFO.

It's clear that the summarized Eigenvalue & the mode shapes of the analyzed system without PSS, the system is sensitive to any disturbance and can easily separate to isolated areas, which exposed the system to blackout.

The using of a different analysis program like the PSAT, which available in [24], or a Power System Toolbox described in [25], Mat-Power [26], Power Analysis Toolbox [27] provided a different Eigenvalues thereby Right & Left Eigenvalue, and participation factor, while it should produce the Eigenvalue within the same trend. That means that all the analysis packages will give that the system has three dominant modes, two-local and one inter-area mode, and the system is unstable as in [28].

4. Optimization Technique

Optimization process applied by two algorithms as follow:

A. Bacterial Foraging

Usual assortment tends to exclude animals with poor foraging strategies (techniques for finding, handling, and feasting food) and favor the propagation of genes of those animals, which have powerful foraging strategies since they have the aptitude to enjoy generative success. After several generations, poor foraging approaches formed into good ones. Rationally, most evolutionary principles attract the scientist to the foraging techniques field to imagine the appropriate foraging activity model as an optimization process [29].

The E. coli bacteria that are existing in our guts also undergo a foraging policy. The control system of these bacteria that dictates how foraging should proceed can be sectioned into four sections as follow [6]:

The chemotaxis step: control system is attained by swimming and tumbling via flagella. Therefore, the E. coli bacterium moves in two different techniques; it can run or tumble, and alternate between these two modes of procedure in the whole epoch. To represent a tumble, a unit length random direction, approximately, ∅_j is generated; this will be used to describe the course of crusade after a tumble [6, 30]. In actual

$$\theta^i(j+1,k,l) = \theta^i(j,k,l) + C(i)\emptyset(j) \tag{7}$$

Where,

$\theta^i(j,k,l)$: is the ith bacterium at jth chemotactic kth reproductive and lth elimination and diffusion phase.

C(i): is the extent of stage occupied in the random way definite by the tumble.

Swarming step: After a group of E. coli cells is positioned in the midpoint of a semisolid agar with a distinct nutrient chemo-effecter (sensor), they goes out from the focus in a traveling circle of cells by moving up the nutrient gradient shaped by feasting of the nutrient by the assembly. Furthermore, if high altitudes of succinate are used as the nutrient, then the cells freedom the attractant aspartate so that they assemble into sets and, hence, move as concentric patterns of groups with high bacterial bulk [30].

The spatial command grades from external movement of the ring and the native releases of the attractant; the cells offer an attraction signal to each other so they swarm together. The swarming exemplified by [30]:

$$J_{cc}\left(\theta, P(j,k,l)\right) = \sum_{i=1}^{S} J_{cc}^{i}\left(\theta, \theta^i(j,k,l)\right) =$$
$$\sum_{i=1}^{S}\left[-d_{attract}exp\left(-\omega_{attract}\sum_{m=1}^{P}\left(\theta_m - \theta_m^i\right)^2\right)\right] +$$
$$\sum_{i=1}^{S}\left[h_{repelent}exp\left(-\omega_{repelent}\sum_{m=1}^{P}\left(\theta_m - \theta_m^i\right)^2\right)\right] \tag{8}$$

Elimination and Dispersal step: like in the residential location, exists of residents of bacteria modifications either progressively or unexpectedly owed to some other effect. Actions befell such that all the bacteria in an expanse die or a set spread into a new fragment of the setting. The bacteria can destroy the chemotactic improvement, also can be assisting

in chemotaxis [30].

B. Modified Particle Swarm Optimization

This process applied by PSO, which considered as an evolutionary system premeditated based on the bird's swarms manners when penetrating food in a search space based on group experience [31]. Many Modifications stratifies on the PSO standard algorithm to improve its searching for the optimum solution like [13].

Reference [32]Modified PSO used to optimize the PID parameter controller in a single machine infinite bus (SMIB). The modifications in the PSO by using the mixture restraining margins condition. This modification mixes the features of the absorbing and reflecting walls. From this proposal, any particle attempt to jump out of the search space in any dimensions, part of the velocity in that dimension absorbed by the boundary. Furthermore, the particle redirected back to the search space with a damped velocity besides a reversal of sign as shown in figure 7.

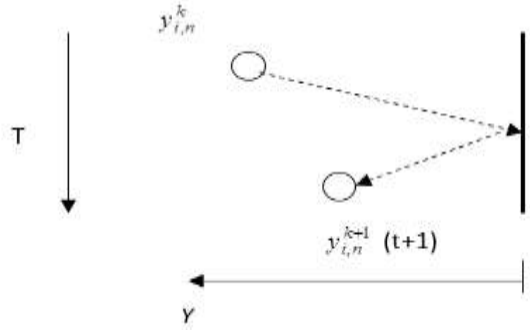

Figure 7. The damping boundary and the reflecting walls.

This process executed in an exact square. First, define the magnitude and sign of the velocity of the reflected particle. Then multiply the speed by a damping factor with a random variable between [0, 1] to produce the restraining effect. Recognize a regularly distributed arbitrary variable between [0, 1]. The proposed behavior damping boundary will lie between the performances of the absorbing and reflecting boundaries [30]. It will work as the absorbing or returning boundary depending on the value of equal to zero or one respectively. The updated velocity of the reduced particle expressed as: -

$$v_{i,n}^{k+1} = \Delta d \times -v_{i,n}^{k+1} \quad (9)$$

Where $v_{i,n}^{k+1}$ denotes the velocity of the imitated particle as if the reflecting boundary forced at the boundary of the search space. In this paper, the damping boundary condition chose to apply it to our problem.

In this paper, the standard PSO toolbox before editing considers as groups of M-files working in the MATLAB background which freely located at the Math-works site [33].

The optimization process depends on the following (A) matrix which computed by state-space analysis from the Heffron–Phillips block diagram of multi-machine power system shown in figure 4 when connected to a lead-lag PSS shown in figure 5. The input of the CPSS is the speed deviation and the output signal of the CPSS used as input to the AVR block.

$$A = \begin{bmatrix} A_{11} & A_{12} & A_{13} & A_{14} \\ A_{21} & A_{22} & A_{23} & A_{24} \\ A_{31} & A_{32} & A_{33} & A_{34} \\ A_{41} & A_{42} & A_{43} & A_{44} \end{bmatrix} \quad (10)$$

$$A_{11}=\begin{bmatrix} 0 & \omega_0 & 0 & 0 & 0 & 0 & 0 \\ \frac{-K_{111}}{M_1} & 0 & \frac{-K_{211}}{M_1} & 0 & 0 & 0 & 0 \\ \frac{-K_{411}}{T'_{do}} & 0 & \frac{-1}{K_{311}T'_{do}} & \frac{1}{T'_{do}} & 0 & 0 & 0 \\ \frac{-K_AK_{511}}{T_A} & 0 & \frac{-K_AK_{611}}{T_A} & \frac{-1}{T_A} & 0 & 0 & \frac{K_A}{T_A} \\ \frac{-K_{111}K_\omega}{M_1} & 0 & \frac{-K_{211}K_\omega}{M_1} & 0 & \frac{-1}{T_\omega} & 0 & 0 \\ \frac{-K_{111}K_\omega T_1}{T_2M_1} & 0 & \frac{-K_{211}K_\omega T_1}{T_2M_1} & 0 & \frac{T_\omega-T_1}{T_2T_\omega} & \frac{-1}{T_2} & 0 \\ \frac{-K_{111}K_\omega T_1T_3}{T_4T_2M_1} & 0 & \frac{-K_{211}K_\omega T_1T_3}{T_4T_2M_1} & 0 & \frac{T_3T_\omega-T_3T_1}{T_4T_2T_\omega} & \frac{T_2-T_3}{T_2T_4} & \frac{-1}{T_4} \end{bmatrix} \quad (11)$$

$$A_{12}=\begin{bmatrix} 0 & \omega_0 & 0 & 0 & 0 & 0 & 0 \\ \frac{-K_{112}}{M_1} & 0 & \frac{-K_{212}}{M_1} & 0 & 0 & 0 & 0 \\ \frac{-K_{412}}{T'_{do}} & 0 & \frac{-1}{K_{312}T'_{do}} & 0 & 0 & 0 & 0 \\ \frac{-K_AK_{512}}{T_A} & 0 & \frac{-K_AK_{612}}{T_A} & 0 & 0 & 0 & 0 \\ \frac{-K_{112}K_\omega}{M_1} & 0 & \frac{-K_{212}K_\omega}{M_1} & 0 & 0 & 0 & 0 \\ \frac{-K_{112}K_\omega T_1}{T_2M_1} & 0 & \frac{-K_{212}K_\omega T_1}{T_2M_1} & 0 & 0 & 0 & 0 \\ \frac{-K_{112}K_\omega T_1T_3}{T_4T_2M_1} & 0 & \frac{-K_{212}K_\omega T_1T_3}{T_4T_2M_1} & 0 & 0 & 0 & 0 \end{bmatrix} \quad (12)$$

$$A_{13}=\begin{bmatrix} 0 & \omega_0 & 0 & 0 & 0 & 0 & 0 \\ \frac{-K_{113}}{M_1} & 0 & \frac{-K_{213}}{M_1} & 0 & 0 & 0 & 0 \\ \frac{-K_{413}}{T'_{do}} & 0 & \frac{-1}{K_{313}T'_{do}} & 0 & 0 & 0 & 0 \\ \frac{-K_AK_{513}}{T_A} & 0 & \frac{-K_AK_{613}}{T_A} & 0 & 0 & 0 & 0 \\ \frac{-K_{113}K_\omega}{M_1} & 0 & \frac{-K_{213}K_\omega}{M_1} & 0 & 0 & 0 & 0 \\ \frac{-K_{113}K_\omega T_1}{T_2M_1} & 0 & \frac{-K_{213}K_\omega T_1}{T_2M_1} & 0 & 0 & 0 & 0 \\ \frac{-K_{113}K_\omega T_1T_3}{T_4T_2M_1} & 0 & \frac{-K_{213}K_\omega T_1T_3}{T_4T_2M_1} & 0 & 0 & 0 & 0 \end{bmatrix} \quad (13)$$

$$A_{14}=\begin{bmatrix} 0 & \omega_0 & 0 & 0 & 0 & 0 & 0 \\ \frac{-K_{114}}{M_1} & 0 & \frac{-K_{214}}{M_1} & 0 & 0 & 0 & 0 \\ \frac{-K_{414}}{T'_{do}} & 0 & \frac{-1}{K_{314}T'_{do}} & 0 & 0 & 0 & 0 \\ \frac{-K_AK_{514}}{T_A} & 0 & \frac{-K_AK_{614}}{T_A} & 0 & 0 & 0 & 0 \\ \frac{-K_{114}K_\omega}{M_1} & 0 & \frac{-K_{214}K_\omega}{M_1} & 0 & 0 & 0 & 0 \\ \frac{-K_{114}K_\omega T_1}{T_2M_1} & 0 & \frac{-K_{214}K_\omega T_1}{T_2M_1} & 0 & 0 & 0 & 0 \\ \frac{-K_{114}K_\omega T_1T_3}{T_4T_2M_1} & 0 & \frac{-K_{214}K_\omega T_1T_3}{T_4T_2M_1} & 0 & 0 & 0 & 0 \end{bmatrix} \quad (14)$$

The (A) matrix can be defined as a diagonal matrix because its diagonal contains the self (A_{ii}) matrix of each machine. The first row of the combined full (A) matrix represents the first generator G1 at A11 and the other generators effects. It's easy to derive the other rows of the (A) matrix as G1.

The (A) matrix used as a MATLAB function, then this function called from the Modified PSO M-files to search for the optimized value of the fifth parameters mentioned in the previous section. Optimized parameters by using Bacterial Foraging and modified PSO shown in table 2.

Table 2. The CPSS optimized parameters by using modified PSO and BG algorithms.

The parameter	Bacterial Foraging	Modified PSO
K_{STAB}	48.6813	47.8804
T_1, T_3	0.036479 Sec.	0.0391 Sec.
T_2, T_4	0.01 Sec.	0.001 Sec.

The optimized gains obtained by relying on a fitness function, which governed by maximizing the smallest damping ratio. This fitness function processed as follows:-

$$mt1 = eig\ (Aa) \tag{15}$$

For mmtt=1:28 (16)

$$\mathrm{mt2(mmtt)} = \frac{-\mathrm{real(mt1(mmtt))}}{\sqrt{\left(\mathrm{real(mt1(mmtt))}^2\right)+\left(\left(\mathrm{imag(mt1(mmtt))}\right)^2\right)}} \tag{17}$$

End

$$md = \min(mt2) \tag{18}$$

$$ma = \max(real(eig(Aa))) \tag{19}$$

Where,

mmtt: is the size of the matrix.

mt1: is the eigenvalues.

mt2: is the damping ratio for each eigenvalue.

md: is the first fitness function which specify the minimum damping ratio.

ma: is the second fitness function which specify the maximum real eigenvalue.

The maximization of the minimum damping ratio applied in the calling of the modified PSO algorithm as:

$$\mathrm{PSOEditing('MFile\ (A\ matrix\ \&\ code)', num.para., [Min.\ \&\ Max.\ values]}$$
$$\mathrm{, (0\ or\ 1) for\ maximizing\ the\ min.\ damping\ ratio\ or\ minimizing\ the\ max.\ real\ part)} \tag{20}$$

This optimized lead-lag PSS by using the modified PSO tested in the multi-machine power system to prove its robustness.

5. Simulation Work

The test procedure established here performed in a simulation manner like a two-area 4-generators 11-bus system problem in a MATLAB/SIMULINK program. SIMULINK file used as an inter-area oscillation studies workbench problem called ("performance of three PSS for inter-area oscillations") shown in Fig. 8. The model data described in [34].

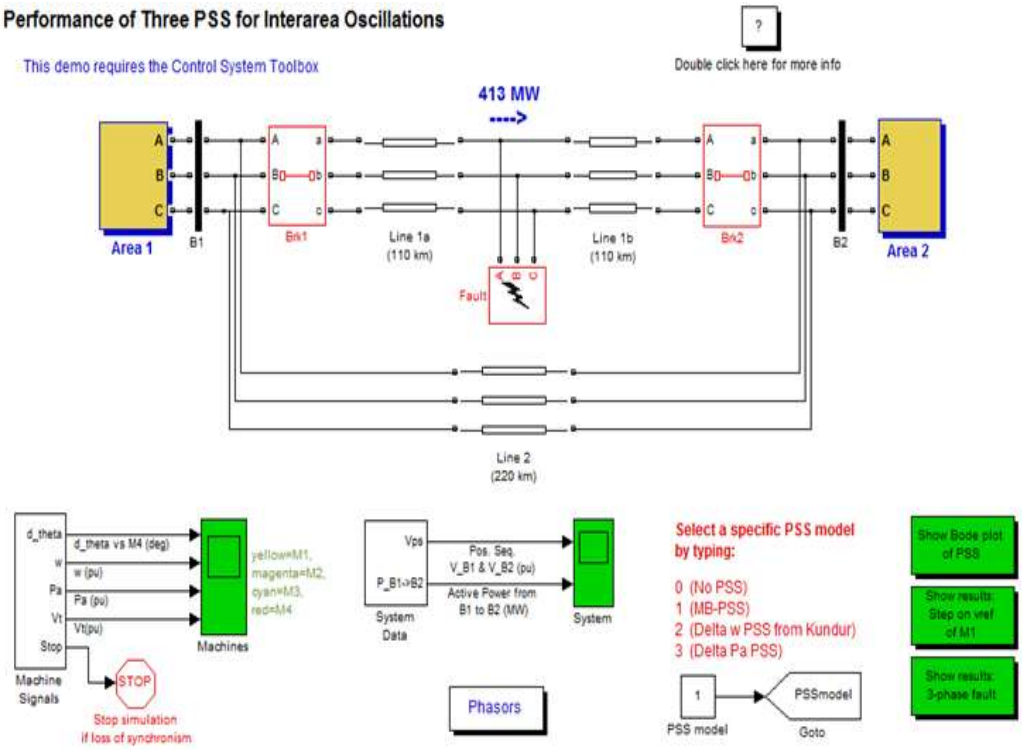

Figure 8. The Simulink multi-machine power system.

The assessment progressions divided into two steps, which proved that the proposed modified PSO based lead-lag PSS is better and more robust than the other compared types in this study.

A. Small signal stability assessment

Small-signal stability test, which considered as the primary objective of the PSS because its proof how fast the PSS damp the inter-area oscillation. Test procedure applied by increasing generator G1 reference voltage by 5% per unit for 12-cycles at 1 Sec. Increasing G1 reference voltage effect on the bulk power transfer from area 1 to area 2 when the system operated without PSS showed in figure 9.

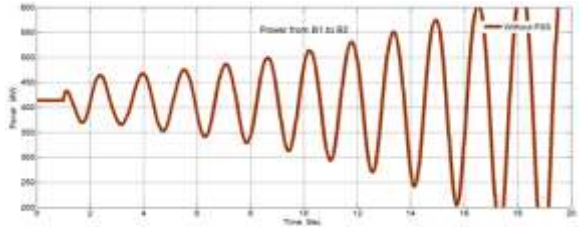

Figure 9. The effect of increasing the voltage magnitude of G1 by 5% for 12-cycles on the bulk power transferred when the system without PSS.

Figure 10 A & B respectively show the G1 the reference voltage increase by 5% effect on all generators speed deviation and terminal voltage without PSS.

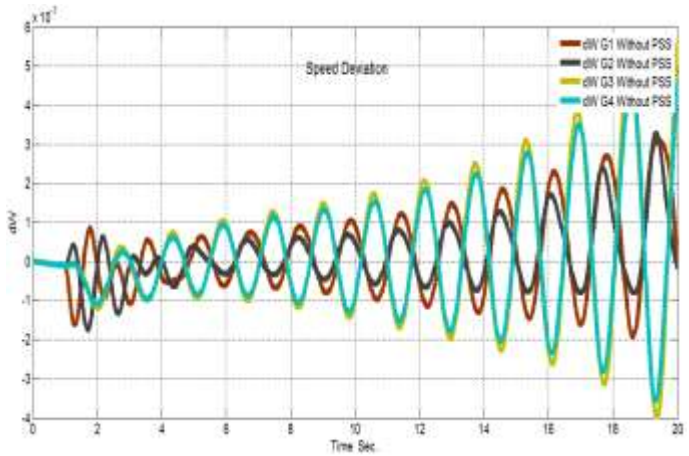

(A)

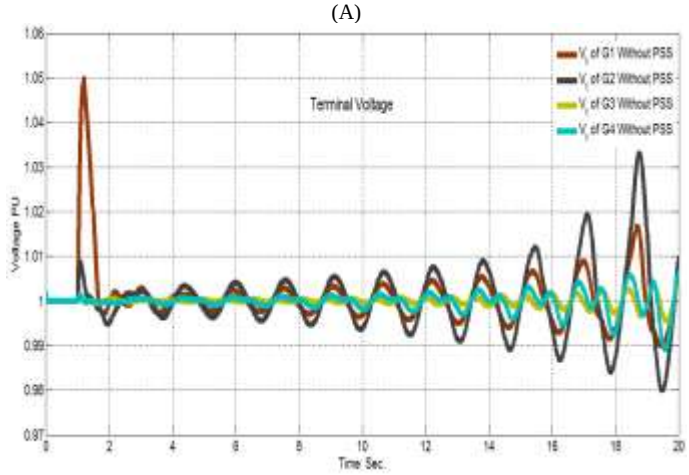

(B)

Figure 10. The response of the system without PSS to the voltage magnitude of G1 increasing by 5% for 12-cycles (A) Speed deviation of the four generators & (B) Terminal voltage of the four generators.

Figures 9 and 10. Proved that the system is unstable as shown previously in the summarized Eigenvalues the system is unstable without PSS. Also, demonstrates that the system AVR and normal excitation without PSS cannot restrain the inter-area oscillation, which makes the system connections between the two areas lost & may lead to the blackout.

This test and the next test will continue to compare the system reaction when connected with the modified PSO based lead-lag PSS, bacterial foraging based lead-lag PSS with the same structure, plus multi-band PSS with simplified settings: IEEE® type PSS4B according to IEEE Std. 421.5. Figure 11 shows the G1 reference voltage increasing by 5% for 12-cycles effect on the bulk power transfer when the system generators connected to PSSs.

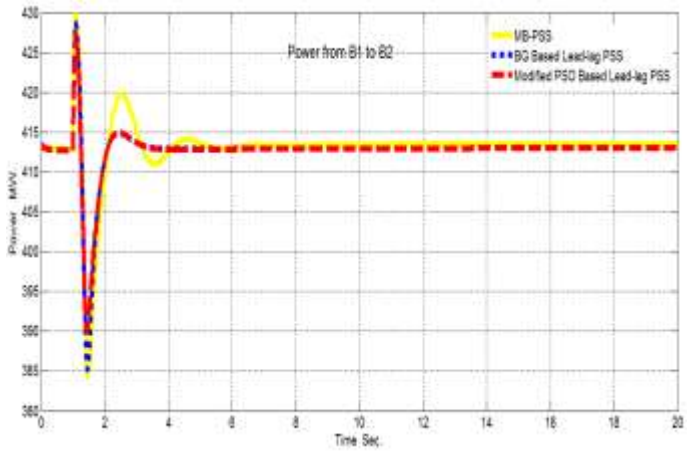

Figure 11. G1 reference voltage magnitude increase by 5% for 12-cycles effect on the bulk power transfer when the system connected to the three compared PSSs.

Table 3 revealed the indices that describe the oscillation of the bulk power transfer from fig. 11.

Table 3. The indices of the bulk power transfer oscillation.

PSS Types	Max. & Min. Overshoots %	Settling Time Sec.	Steady-State Error %
MB-PSS	+4.0224% -35.8510%	5.9450	+0.1286%
BG Based lead-lag PSS	+3.7961% -6.7300%	3.0601	+0.0020%
Modified PSO Based lead-lag PSS	+3.5058% -5.5513%	3.1037	+0.0020%

Figure 11 and its characteristic in Table 3 demonstrates that the maximum overshoot of the proposed modified PSO Based lead-lag PSS is the smallest. Also, the power in the other two PSSs cases tumbles in a broader extent than the modified PSO based lead-lag PSS. While the steady-state errors of the modified PSO equal the BG based lead-lag PSS, but still the proposed PSS is robust from the point of representation of maximum & minimum overshoots.

Figure 12 displays the G1 speed deviations responses through the G1 reference voltage increase by 5% for 12-cycles when the system connected upon the compared controls. Table 4 shows the indices that investigate the oscillations.

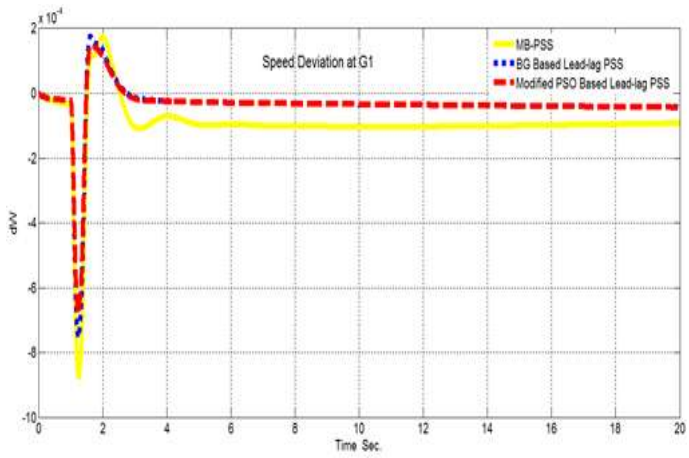

Figure 12. G1 speed deviation response to G1 reference voltage magnitude increase by 5% for 12-cycles when the system equated to the three compared PSSs.

Table 4. The speed deviations oscillations characteristics.

PSS Types	Max. & Min. Overshoots	Settling Time Sec.	Steady-State Error
MB-PSS	+1.748e-4 -8.7674e-4	4.3624	-9.2822e-5
BG Based lead-lag PSS	+1.751e-4 -7.557e-4	5.8994	-4.8344e-5
Modified PSO Based lead-lag PSS	+1.494e-4 -6.825e-4	4.1923	-4.4e-5

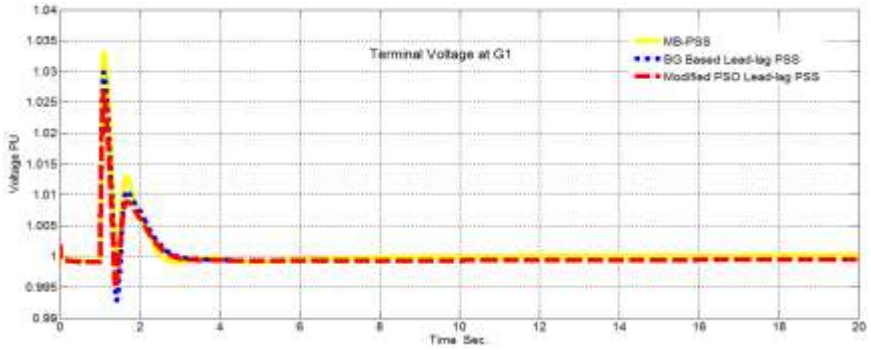

Figure 13. The G1 voltage magnitude increase by 5% for 12-cycles effect on the G1 terminal voltage when the system connected to the three compared PSSs.

Figure 12 presents the G1 speed deviation of the small-signal test, which proves the superiority of the proposed PSS to the other PSS. Similarly, the characteristic of the figure that explained in table 4 revealed the suggested modified PSO constructed lead-lag PSS has, the less

settling time, steady-state error, and hesitating in the small band. This information proves that the proposed PSS better than the other PSSs at limiting the oscillations.

Figure 13 represents the G1 reference voltage increase by 5% per unit for 12-cycles influence on the G1 terminal voltage when the system connected to the three PSSs. Table 5 indicates the indices that exemplify figure 13.

Table 5. The g1 terminal voltage oscillation characteristics.

PSS Types	Max. & Min. Overshoot P.U.	Settling Time Sec.	Steady-State Error P.U.
MB-PSS	1.0330 0.9970	5.8000	1.0001
BG Based lead-lag PSS	1.0299 0.9929	2.9182	1.00001
Modified PSO Based lead-lag PSS	1.0267 0.9949	2.8352	1.000005

Figure 13 and table 5 verified that the effect of the step response to the G1 terminal voltage in case of the proposed modified PSO lead-lag PSS is less than the other two PSSs.

It's known that the fundamental objective of the PSS is to restrain the small-signal oscillations. So, the better controller in damping the LFOs in this test proves that this controller is robust. Besides, this comparison declares that the proposed PSS damp the inter-area uncertainty toward the small-signal oscillation better than the other two PSSs.

The next test used to show how the proposed PSS robust & superior to the other PSSs in restraining the oscillation counter to short-circuit examine. Proposed modified PSO based lead-lag PSS improves the system reaction to the small signal stability over than the MB-PSS by (113.096%), and superior to the BG based lead-lag PSS (30.54%).

B. Large signal assessment

The superiority of the proposed PSS will be checked in this valuation when compared with the other two PSSs. The test procedure three-phase short-circuit in one of the two parallel middle 220Km lines, which connect area 2 with area 1 and transfer (413MW). Then the fault cleared by the circuit breaker (1, 2) after 8-cycles and C.B (1,2) opens the faulted line, but the two regions still connected through the second line.

The system returns after the short circuit into a new operating point. The PSS damp the oscillations after clearing the fault, which considers as a high strength test to the proposed modified PSO based lead-lag PSS.

Figure 14 displays the 8-cycles three-phase short-circuit effect on the bulk power transferred from the area (1) to the region (2) when the system connected to the MB-PSS, BG based lead-lag PSS, and proposed modified PSO based lead-lag PSS. Table 6 indicates the characteristics of fig. 14.

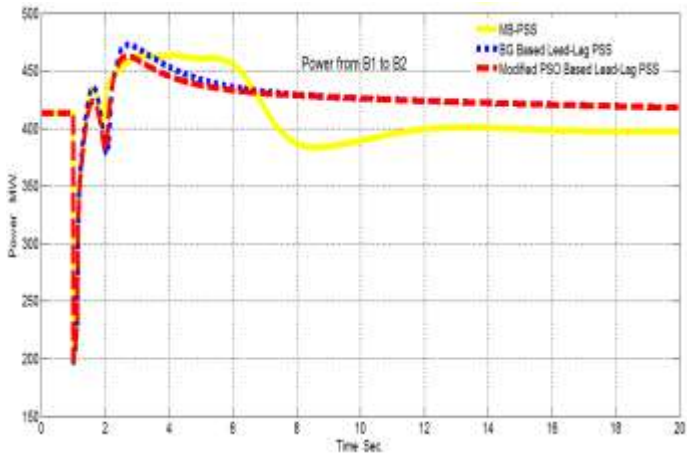

Figure 14. The 8-cycles three-phase fault clearing effect on the bulk power transferred when the system connected to the three PSSs.

Table 6. The characteristics of the bulk power transfer oscillation.

PSS Types	Max. & Min Overshoot MW	Settling Time Sec.	Steady-State Error %
MB-PSS	+12.2929% -52.47%	10.6787	-3.8354%
BG Based lead-lag PSS	+14.3543% -8.6722%	13.6240	+1.1792%
Modified PSO Based lead-lag PSS	+11.9746% -7.6474%	13.7083	+1.1308%

The three-phase SC effect on the bulk power transferred. Depicts that the MB-PSS with the lower settling time, but it pauses in a large variety with the highest maximum overshoot, and the worst its steady-state error. It indicates that the MB-PSS is the weakest in damping the oscillation. On the other hand, the proposed modified PSO based lead-lag PSS reaction has the lowest maximum overshoot, wavering in a small band, and the least steady-state error, which makes the proposed PSS better than the other in conflict this test and in clearing the Short-circuit effect on the bulk power transferred between the two areas.

Figure 15 illustrates the G1 speed deviations response to three-phase SC. When the system connected to the three PSSs. Table 7 characterizes the speed deviations response.

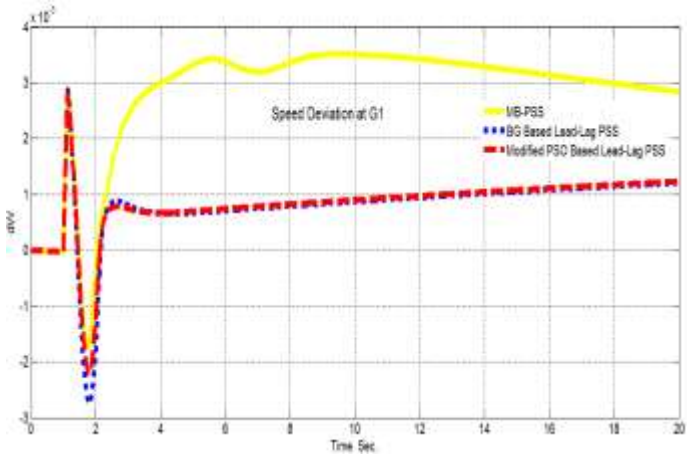

Figure 15. The system speed deviation response of clearing three-phase fault after 8-cycles when the system connected the three PSSs.

Table 7. The characteristics of the speed deviation oscillation.

PSS Types	Max. & Min Overshoot	Settling Time Sec.	Steady-State Error
MB-PSS	0.0035 -0.0017	18.7186	2.8374e-3
BG Based lead-lag PSS	0.0029 -0.0028	17.4077	1.203e-3
Modified PSO Based lead-lag PSS	0.0028 -0.0022	17.7276	1.2285e-3

The speed deviation response of the system, when connected to the proposed PSS has, the less maximum overshoot, less vacillating band, and moderate steady-state error in comparison to the other PSS.

Figure 16 indications the effect of the three-phase SC. On the G1 terminal voltage when all generators in the system connected to the three compared PSSs. Table 8 analyzes the G1 terminal voltage deviation.

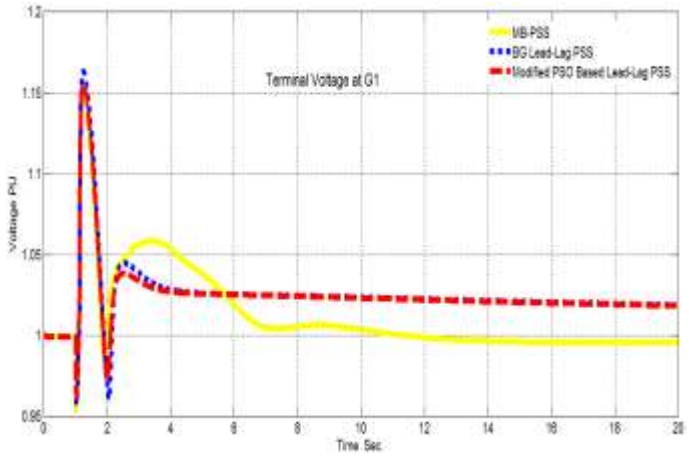

Figure 16. The three-phase fault clearing after 8-cycles effect on the terminal voltage of generator G1 when the system connected the three PSSs.

Table 8. G1 terminal voltage oscillation characteristics.

PSS Types	Max. & Min Overshoot	Settling Time Sec.	Steady-State Error
MB-PSS	1.1510 0.9536	11.9181	0.992
BG Based lead-lag PSS	1.1634 0.9606	12.5431	1.0186
Modified PSO Based lead-lag PSS	1.1555 0.9727	12.0683	1.0183

The proposed PSS performance supports the system to remove the S.C. effect. It's clear that the proposed modified PSO based lead-lag PSS robust and superior to the other PSS in limiting the oscillations and return the system to a stable region with a new operating point.
Proposed modified PSO based lead-lag PSS improves the system response to counter out the large signal short-circuit test higher than the MB-PSS by (75.2967%), and higher than the BG based lead-lag PSS by (15.5167%).

At the end of this study the editing of the PSO, which make it better at optimizing the gains of the lead-lag PSS. It results in that the optimized PSS in this proposal can restrain the inter-area oscillation robust than the other PSSs and increase the overall system stability. Also, the proposed modified PSO based lead-lag PSS when connecting to the system strongly suppresses the LFOs and faster than the other compared PSSs.

6. Conclusion

In this study, the editing particle swarm optimization (PSO) boundary makes it as a reflecting and absorbing wall, which prevents the particle from exiting the search space. The adjustment makes the PSO better choosing and optimizing the power system stabilizer (PSS) gains.
The proposed modified PSO used to optimize the lead-lag P. Kundur structure with speed deviation as the input signal. This proposed PSS compared with bacterial foraging based the same lead-lag PSS, and the multi-band PSS.

An optimization process depending on two-fitness functions, maximizing the minimum damping ratio and the minimizing of the maximum real-part of Eigenvalues. Applying maximization of the damping ratio makes the optimization process yields a better result.

Comparison process between the proposed modified PSO based lead-lag PSS and the compared PSSs applied in a two-area 4-generators 11-bus workbench examination system. The assessments compromise two steps small-signal test through increasing the G1 reference voltage by 5% per unit for 12-cycles, and large-signal test among three-phase short-circuit for 8-cycles.

Oscillation effect on the bulk power transfer, generator G1 speed deviations, and voltage terminal estimates by Eigenvalues, participation factors, damping ratios, settling times, steady state errors indices.

The study of the effects of the three compared PSSs admits that the proposed modified PSO based lead-lag PSS robust and superior to the other associated PSSs.

Performance comparison of the three PSSs in this study proves that the proposed modified PSO based lead-lag PSS develops the overall system stability when damping the inter-area oscillation effectively and eliminate the effects of large and small tests faster than the analyzed two PSSs.

7. References

[1] M. A. Hannan, N. N. Islam, and etc., "Artificial Intelligent Based Damping Controller Optimization for the Multi-Machine Power System: A Review," *IEEE Access* , vol. 6, pp. 39574 - 39594, 13 Jul. 2018.

[2] P. Kundur, J. Paserba, and etc. , "Overview on definition and classification of power system stability," in *CIGRE/IEEE PES Inter. Sympo. Qual. and Secu. of Elec. Power Deli. Sys., 2003. CIGRE/PES 2003.*, Montreal, Quebec, Canada, Canada, 8-10 Oct. 2003..

[3] L. L. GRIGSBY, Power System Stability and Control, Boca Raton, USA: CRC Press, Taylor & Francis Group, 2012.

[4] I. Erceg, D. Sumina, and etc., "Power system stabilizer based on pointwise min-norm control law," *Elec. Power Sys. Rese.*, vol. 143, pp. 215-224, Feb. 2017.

[5] A. Faraha, T. Guesmi, and etc., "A new method for the coordinated design of power system damping controllers," *Eng. App. of Artif. Inte.*, vol. 64, pp. 325-339, Sep. 2017 .

[6] B. Khorram, and H. Lesani, "Coordinated Control of Flexible AC Transmission System Devices and Power System Stabilizer for improve the Power System Stability Using," *Inter. Jour. on Elec. Eng. & Informatics IJEEI*, vol. 7, no. 2, June, 2015.

[7] A. K. Patra, S. K. Mohapatra, and etc., "Application of firefly based for coordinated design of PSS and PID based SSSC-based controller," in *2018 Tech. for Smart-City Ener. Sec. & Power (ICSESP)*, Bhubaneswar, India, 28-30 Mar. 2018.

[8] A. Sallama, M. Abbod, and etc., "Supervisory Power System Stability Control using Neuro-fuzzy system and particle swarm optimization algorithm," in *2014 49th Inter. Uni. Power Eng. Conf. (UPEC)*, Cluj-Napoca, Romania, 2-5 Sept. 2014.

[9] M. Ahmed, and N. K. Roy, "Design of a power system stabilizer using adaptive-neuro fuzzy logic for a multi-machine system having dynamic loads," in *2016 5th Int. Conf. on Infor., Electr. & Vision (ICIEV)*, Dhaka, Bangladesh, 13-14 May 2016.

[10] S. Bhattacharya, "Power system oscillation damping by intelligent power system stabilizer," in *2016 IEEE 1st Inter. Conf. on Power Electr., Intel. Control & Ener. Sys. ,* (ICPEICES), Delhi, India, 4-6 Jul. 2016.

[11] K.R. Sudha, V. S. Vakula, and etc., "Particle Swarm Optimization in Fine Tuning of PID Fuzzy Logic Power System Stabilizer," in *2009 Inter. Conf. on Advan. in Compu., Control, & Teleco. Tech.*, Trivandrum, Kerala, India, 28-29 Dec. 2009.

[12] A. Jalilvand, R. Aghmasheh, and etc., "Robust design of PID power system stabilizer in multi-machine power system using artificial intelligence techniques," in *2010 4th Inter. Power Eng. & Opti. Conf. (PEOCO)*, Shah Alam, Malaysia, 23-24 Jun. 2010..

[13] H. Gadari, "HPSO algorithm to design power system stabilizer in multi-machine power system," in *8th Inter Conf on Power Electr. - ECCE Asia*, Jeju, South Korea, 30 May-3 June 2011.

[14] Ravindrababu M., G. Saraswathi, and K. R. Sudha, "Design of Firefly Based Power System Stabilizer Based on Pseudo Spectrum Analysis," *Inter. Jour. on Elec. Eng. and Informatics (IJEEI)* , vol. 9, no. 1, March 2017.

[15] H. K. Abdulkhader, J. Jacob, and etc., "Fractional-order lead-lag compensator-based multi-band power system stabiliser design using a hybrid dynamic GA-PSO algorithm," *IET Gene. Trans. & Distr.*, vol. 12, no. 13, pp. 3248 - 3260, 19 Jul. 2018.

[16] R. Hemmati, "Power system stabilizer design based on optimal model reference adaptive system," *Ain Shams Eng. Jour.*, vol. 9, no. 2, pp. 311-318, Jun. 2018.

[17] P. Kundur, Power System Stability and Control, New York, USA: McGraw-Hill, Inc., 1994.

[18] A.R.Fereidounia, B.Vahidi, and etc., "Improvement of low frequency oscillation damping by allocation and design of power system stabilizers in the multi-machine power system," *Inter. Jour. of Elec. Power & Ener. Sys.*, vol. 52, pp. 207-220, Nov. 2013.

[19] I. C. Report, "Dynamic Models for Steam and Hydro Turbines in Power System Studies," *IEEE Trans. on Power Appar. & Sys.*, Vols. PAS-92, no. 6, pp. 1904 - 1915, Nov. 1973.

[20] I. Editors, "421.5-2005- IEEE Recommended Practice for Excitation System Models for Power System Stability Studies," IEEE, 21 Apr. 2006.

[21] Y. Y. Hsu, and C. L. Chen, "Identification of optimum location for stabiliser applications using participation factors," *IEE Proc. C - Generation, Transm. & Distr.*, vol. 134, no. 3, pp. 238 - 244, May 1987.

[22] F. P. Demello, and C. Concordia, "Concepts of Synchronous Machine Stability as Affected by Excitation Control," *IEEE Trans. on Power Appar. & Sys.*, Vols. PAS-88, no. 4, pp. 316 - 329, Apr. 1969.

[23] Y. Anantholla, and K. N. Shubhanga, "Manual for A Multi-machine Smallsignal Stability Programme," Department of Electrical Engineering, IIT Bombay, 29 Jan. 2009. [Online]. Available: https://www.ee.iitb.ac.in/~peps/downloads.html. [Accessed 1 Aug. 2018].

[24] F. Milano, "Federico Milano's Webpage," University College Dublin, 6 Jan. 2013. [Online]. Available: http://faraday1.ucd.ie/psat.html. [Accessed 1 Jan. 2018].

[25] J.H. Chow, and K.W. Cheung, "A toolbox for power system dynamics and control engineering education and research," *IEEE Trans. on Power Sys.*, vol. 7, no. 4, pp. 1559 - 1564, Nov. 1992.

[26] R. D. Zimmerman, C. E. Murrillo-Snchez, and D. Gan., "MatPower, Version 3.0.0, Users Manual," Power Sys. Eng. Rese. Center, Cornell Univ., Ithaca, New York, 2005.

[27] K. Schoder, A. Hasanovic, and etc., "PAT: a power analysis toolbox for MATLAB/SIMULINK," *IEEE Trans. Power Sys.*, vol. 18, no. 1, pp. 42-47, 19Feb. 2003.

[28] A. V. Ubisse, K. A. Folly, and etc., "Comparison of Matlab PST, PSAT and DigSILENT for transient stability studies on parallel HVACHVDC transmission lines,," in *45th Inter. Univ. Power Eng. Conf. UPEC2010*, Cardiff, Wales, U.K., 31 Aug.-3 Sept. 2010.

[29] K. Passino, "Biomimicry of bacterial foraging for distributed optimization and control," *IEEE Cont. Sys. Magaz.*, vol. 22, no. 3, pp. 52 - 67, 07 Aug. 2002.

[30] S. Mishra, "A hybrid least square-fuzzy bacterial foraging strategy for harmonic estimation," *IEEE Trans. on Evolut. Computa.*, vol. 9, no. 1, pp. 61 - 73, 22 Feb. 2005.

[31] P. K. Ray, S. R. Paital, and etc., "Swarm and bacterial foraging based optimal power system stabilizer for stability improvement," in *2016 IEEE Region 10 Conf. (TENCON)*, Singapore, Singapore, 22-25 Nov. 2016.

[32] Nader M.A. Ibrahim, Hossam E. M. Attia, and etc., "Modified particle swarm optimization based proportional-derivative power system stabilizer," *I.J. Intel. Sys. & App. (IJISA)*, vol. 7, no. 3, pp. 62-76, Feb. 2015.

[33] B. Brige, "Particle Swarm Optimization Toolbox," MathWorks, 20 Mar. 2006. [Online]. Available: https://www.mathworks.com/matlabcentral/fileexchange/7506-particle-swarm-optimization-toolbox. [Accessed 2018 Aug 10].

[34] M. Klein, G. J. Rogers, and etc., "Analytical investigation of factors influencing PSS performance," *IEEE Trans. on EC*, vol. 7, no. 3, pp. 382-390, Sep. 1992.

Nomenclature:

$\delta^{'}$: The differentiation of rotor angle deviation in elec. Rad.

ω_r : Rotor speed.

ω_0 : The rated rotor speed in elec. Rad /sec.=2 $2\Omega f_0$

P_m : The mechanical power.

P_e **:** Electrical power

D **:** Damping coefficient**.**

K_D **:** Damping constant.

M **:** Inertia coefficient.

$e_q^{'} - e_d^{'}$: Differentiation of (q & d)-axis transient voltage respectively.

$X_d - X_q$: (d & q)-axis synchronous reactance respectively.

$X_d^{'} - X_q^{'}$: (d & q)-axis transient reactance respectively.

$T_{do}^{'} - T_{qo}^{'}$: (d & q)- axis open circuit transient time constant respectively.

$T_{do}^{''} - T_{qo}^{''}$: (d & q)- axis open circuit sub-transient time constant respectively.

$i_d - i_q$: The stator phase currents of dq transformation.

$K_1 : K_6$ **:** Constants of the linearized model of synchronous machine.

U : The vector of inputs to the system

Δ : Linearized incremental quantity

T_M : Mechanical torque.

K_A : Voltage regulator gain.

T_A : Voltage regulator time constants.

K_{STAB} : Lead-lag stabilizer gain.

$T_1 : T_4$: Lead-lag controller time constants.

T_{CH} : Steam chest time constant.

T_{RH} : Reheat time constant.

T_{CO} : Crossover time constant.

F_{HP} : High pressure turbine power fraction.

F_{IP} : Intermediate pressure turbine power fraction.

F_{LP} : Low pressure turbine power fraction.

P_{GV} : Power at gate or valve outlet.

P_0 : Initial mechanical power of the speed governor.

$P_{UP}^{\cdot} - P_{DOWN}^{\cdot}$: Limits of rate of change of power imposed by control valve rate limits.

$P_{MAX} - P_{MIN}$: Power limits imposed by valve or gate travel.

K : Total effective speed governing gain.

S : Laplace operator.

Nader M.A. Ibrahim was born in Alexandria in Egypt, on 13 October, 1986. He received his B.Sc. & M.Sc. degrees in electrical power systems and machines department in Faculty of Industrial Education from Suez Canal University, Suez, Egypt during 2009 and 2015 respectively. Eng. Nader registered PhD in electrical power systems and machines control. Currently, he is Assistant Lecturer in electrical department at the Faculty of Industrial Education, Suez University, Suez, Egypt. His research interests are power system stability and operation, machine control, wide-area damping control, online and digital control in machines, applications of artificial intelligent techniques, like particle swarm optimization (PSO).

Basem E. Elnaghi received the B.Sc. degree in electrical engineering from Suez Canal University, Port Said, Egypt, in 2003, the M.Sc. degree in electrical engineering from Suez Canal University, Port Said, Egypt, in 2009, and the Ph.D. degree in electrical engineering from Port Said University, Port Said, Egypt, in 2015. He is currently an Assistant Professor in the Electrical Engineering Department, Suez Canal University, Ismailia, Egypt.

Hamed A. Ibrahim Emam received the B.Sc. and M.Sc. degree in electronic engineering from Menofia University, El- Menofia, Egypt in 1992 and 2001 respectively. Dr. Hamed received the Ph. D. degree from Université de Versailles, France in 2010. He is a member of Faculty of Industrial Education, Suez University, Suez, Egypt since 2010 until now. His research interests are in the area of renewable energy sources, power electronics, dynamic modeling, robotic, fuzzy systems, and neural network.

Hossam E.A. Talaat received the B.Sc. and M.Sc. degrees from Ain Shams University, Cairo, Egypt in 1975 and 1980 respectively, and his Ph.D. degree from University of Grenoble, France in 1986. During 1999-2001. He is a reviewer of many international journals (IEEE, IET, Electric Power System Research, Electrical power and Energy systems, ...). He has supervised 40+ Ph.D. and M.Sc. theses in the field of power system operation, control, stability and protection. He has taught tens of undergraduate and graduate courses in this field. He has authored and co-authored more than 70 technical papers and reports. He has accomplished several research projects as PI and as the investigator. He was the reviewer of a number of academic undergraduate and postgraduate programs for Egyptian and Arabic Universities. He is the Chairman of 2 IEC committees (49&93) and was a member of the Egyptian National board of Electricity and Energy Researches– Scientific Research and Technology Academy. He is the Chairman of the Middle East Conference on Power Systems MEPCON 2014 to be held on 23th-25th December 2014. He is interested in many research areas such as: Distributed Generation and Micro grids, Application of artificial intelligence techniques (Neural Networks, Knowledge-Based systems, Genetic Algorithms, and Fuzzy Logic) to Power System analysis, control, and protection; Real time applications to electrical power systems and machines; Application of optimal and adaptive control techniques for the enhancement of power system stability.